Research Article

Masudulla Khan, Azhar U. Khan, Il Soo Moon, Raed Felimban, Raed Alserihi, Walaa F. Alsanie, and Mahboob Alam*

Synthesis of biogenic silver nanoparticles from the seed coat waste of pistachio (*Pistacia vera*) and their effect on the growth of eggplant

https://doi.org/10.1515/ntrev-2021-0107
received August 11, 2021; accepted October 4, 2021

Abstract: Herein, the synthesis of silver nanoparticles using extracts of pistachio seed coat waste is investigated. The surface plasmon resonance peak at 443 nm was observed in the nanoparticles by using ultraviolet-visible spectroscopy (UV-Vis). To identify potential biomolecules involved in the bio-reduction of silver ions, Fourier-transform infrared spectroscopy (FTIR) was used. Scanning and transmission electron microscopy (SEM and TEM) show irregular shapes with an average size of ~20 nm. The active surface determined by Brunauer, Emmett, and Teller analysis was 22 m^2/g. The effect of silver nanoparticles on eggplants sprayed with a nanoparticle suspension of 75 mg/L led to increased plant growth and chlorophyll and carotenoid contents. The fly ash addition to the soil promoted plant growth. The highest increase in plant growth occurs when plants were sprayed with 75 ppm AgNPs in 20% fly ash amended soil.

Keywords: biogenic synthesis, silver nanoparticles, eggplant, application

* **Corresponding author: Mahboob Alam,** Division of Chemistry and Biotechnology, Dongguk University, Gyeongju, 780-714, Republic of Korea, e-mail: mahboobchem@gmail.com
Masudulla Khan: Department of Botany, Aligarh Muslim University, Aligarh 202002, India
Azhar U. Khan: Department of Chemistry, School of Basic Sciences, SIILAS CAMPUS, Jaipur National University, Jaipur, Rajasthan 302017, India
Il Soo Moon: Department of Anatomy, Dongguk University College of Medicine, Gyeongju, 38066, Republic of Korea
Raed Felimban, Raed Alserihi: Department of Medical Laboratory Technology, Faculty of Applied Medical Science, King Abdulaziz University, Jeddah, Saudi Arabia
Walaa F. Alsanie: Department of Clinical Laboratory Science, Faculty of Applied Medical Science, Taif University, Taif, Saudi Arabia

1 Introduction

Nanotechnology has emerged in recent years as one of the most important areas of modern science associated with green synthesis [1]. The use of modern techniques to synthesize nanoparticles has become a popular application for a variety of products in the biomedical and healthcare fields [2]. Richard Feynman coined the term "nanotechnology" for the first time in 1959, which is widely regarded as the start of modern nanotechnology [3]. The green synthesis approach has been subjected to a reliable, sustainable, and eco-friendly protocol to synthesize a variety of nanoparticle metal oxides and metal oxides in some cases under exposure to solar radiation to accelerate the synthesis of nanoparticles. A great deal of attention has been paid in recent years to the exploration of waste materials in different areas of human application. One of these areas where scientists focus with zeal [4,5] is the use of plant waste materials with different names such as shell, seed coat fruit peel, skin, hull, *etc*., containing bioactive compounds [6]. These waste materials are a prime example of an undervalued and unused energy source that can be used as a reducing agent in nanoparticle synthesis. The list of waste materials of plants used for silver nanoparticles synthesis and their particle size is given in the Supplementary Information (Table S1). Due to their unique characteristics, nanoparticles are used in many industrial sectors. Of the various types of nanoparticles, silver nanoparticles (AGNPs) are the most commonly used [7–9]. Synthesis of nanoparticles from plant parts is preferred because it is simple, environment friendly, and safe [10,11]. The plant materials are more advantageous, feasible, and simple for nanoparticles synthesis than other materials [12,13]. The use of nanoparticles to enhance plants growth is currently being researched all over the world [14]. Silver nanoparticles (AgNPs) have antimicrobial, catalytic, physiochemical, and optical properties [15]. Brinjal (*Solanum*

melongena L.) is a popular nightshade crop grown all over the world. It is one of the most common and widely consumed vegetables in India. In this country, 730,000 hectares of land are under eggplant cultivation with an annual production of 12,801 million tonnes [16]. Metal-based nanomaterials are being developed by scientists to aid plant growth and development. Nanotechnology has the potential to be a useful tool for delivering pesticides and fertilizers to the target site with accuracy and precision. Nanoparticles injected into plants could have a significant impact, and thus, could be used to improve plant growth and yield in agricultural applications [17]. However, more research work is needed to fully comprehend the molecular mechanism of action of nanoparticles in plant physiology [18]. Plants have been found to be capable of producing the natural mineralized nanomaterials required for their growth under certain conditions [19]. To the best of our knowledge, this is the first study to use aqueous seed coat extract of pista (*Pistacia vera*) to the biosynthesis of AgNPs as part of a green nanoparticle synthesis approach. The novelty of this article is therefore to describe the green synthesis of AgNPs from the waste part of the seed and to investigate their impact on eggplant plant growth capacity, carotenoid, and chlorophyll content.

The seed coat extract of pista (*Pistacia vera*) was used to synthesize silver nanoparticles (AgNPs). The material was cleaned with distilled water to remove contaminated contents and air-dried in sunlight. The material was ground into a fine powder, and 20 g of the fine powder was placed in a flask with 200 mL double distilled water, which was then refluxed for 30 min. For the next step, the plant extract was cooled and filtered through Whatman filter paper no. 1.

As such, silver nitrate GR was used, which was obtained from Merck (India). In an Erlenmeyer flask, 100 mL of silver nitrate at a concentration of 1 mM was prepared. Then, various concentrations of the seed coat extract (2.5, 5.0, and 10 mL) were added to 90 mL of silver nitrate solution to optimize the rapid reduction of $AgNO_3$ and left at room temperature to observe the color change; the formation was also recognized by using UV-Visible spectroscopy in the range of 443 nm. Centrifugation at 10,000 rpm for 20 min was used to collect biosynthesized AgNPs, which were then carefully washed with double-distilled sterile water. The collected nanoparticles synthesized using 10 mL of the extract based on the rapid reduction of $AgNO_3$ to AgNPs were further investigated by using FT-IR, XRD, UV-Vis, SEM, and TEM spectroscopic techniques.

2 Materials and methods

2.1 Biosynthesis of silver nanoparticles and characterization

Silver nanoparticles were synthesized using the same protocol as in prior research [10,20]. All other chemicals such as sodium hypochlorite (NaOCl), silver nitrate ($AgNO_3$), and the solvents and chemicals used in this study were provided by Merck India Ltd. UV-Vis spectral analysis was used to validate the production of AgNPs using a Shimadzu spectrophotometer UV-Vis 1800 (Japan). Cu K radiation (λ = 0.15405 nm) was used for X-ray diffraction (XRD, PANalytical, X'pert PRO-MPD, The Netherlands). SEM (NOVA nano FE-SEM 450 FEI) and TEM (TECNAI-G-20). were used to examine the morphology and the size of the prepared AgNPs. FT-IR spectra of the plant extract and biosynthesized AgNPs were collected utilizing the KBr pellet technique with PerkinElmer Spectrum 2000 in the 4,000–400/cm range. The specific surface area of biogenic silver nanoparticles using nitrogen adsorption–desorption isotherms (Brunauer–Emmett–Teller (BET)) was calculated with the Nova 3200e.

2.2 Plant culture, total leaf chlorophyll, and the carotenoid content

Eggplant seeds were sterilized for 5 min with 0.1% sodium hypochlorite and then washed twice with distilled water. Fifteen days old seedlings of eggplant were sprayed with biosynthesized AgNPs and one set of plants was left without spraying as control (without AgNPs). Each treatment had five replicates. The experiment results were terminated 100 days after spraying of AgNPs.

The total chlorophyll and carotenoid content of photosynthetic pigments of eggplants were approximated using the method given by Mackinney [21] and Maclachlan and Saul [22], respectively.

2.3 Fly ash

In this experiment, we used loam soil, which was obtained from the fields of Jaipur, India.

Before planting, the soil was autoclaved at 137.9 kPa for 20–25 min, while the fly ash was sun-dried for 10–15 days

and mixed (vol:vol) in four proportions with soil: 0 (100), 20, 50, and 100% fly ash. About 3 kg of fly ash and soil mixtures were placed in pots. Fly ash was purchased from a local market in Jaipur, India.

2.4 Statistical analysis

The data were analyzed using ANOVA in GraphPad Prism software, and means were compared using mean and standard deviation including the Tukey *post-hoc* test and Dunnett's multiple comparisons test at the $p < 0.05$ probability level. The mean and standard deviation presented in the graph was designed using Excel software.

3 Results and discussion

Previous research studies have reported on the biosynthesis of silver nanoparticles from plant parts [10,11,20]. Therefore, in continuation with our interest in the preparation of silver nanoparticles from the seed coat waste extract of pista, in the current research, AgNPs have been prepared and their impact on eggplant plants is studied.

3.1 Fourier infrared spectroscopy analysis (FTIR)

FT-IR spectra of the biogenic synthesis of Ag-nanoparticles and the aqueous extracts of *Pistachio* shells are displayed in Figure 1. FT-IR spectra of plant extracts (Figure 1a)

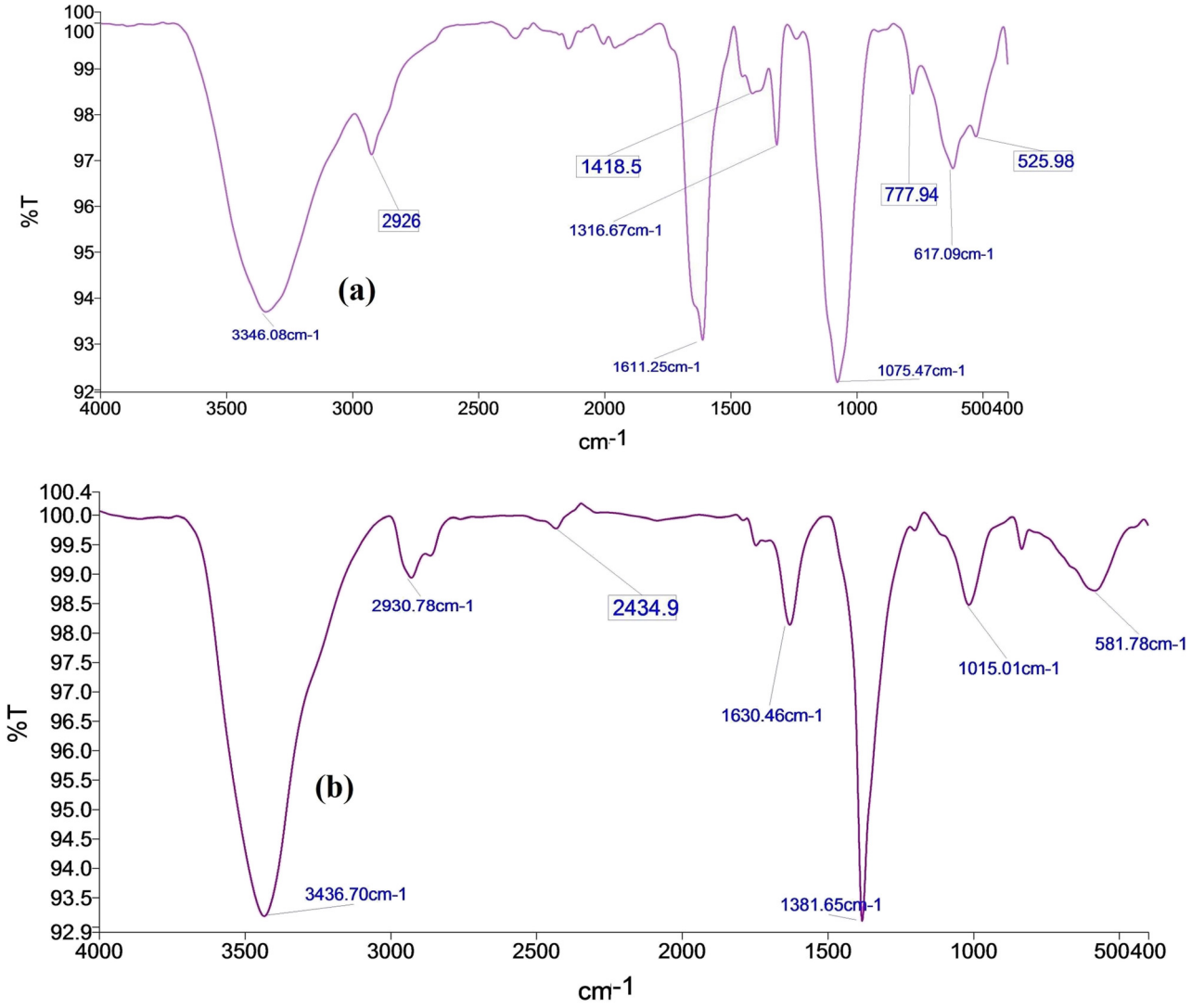

Figure 1: FT-IR spectra of the (a) extract of pista and (b) biosynthesized AgNPs.

and AgNPs were used to identify the metabolites responsible for Ag ion reduction (Figure 1b). Typical infrared absorption bands at 3446.08 and 3436.70/cm showed an indication of the presence of phenol and alcohol with a free functional group (–OH) [23]. The wide infrared bands of the OH group, generally as shown in Figure 1, were overlaid with the NH stretching band [24]. The absorption bands reflected the presence of alkanes (methyl and methylene groups) in the lipids indicating asymmetric stretching bands at 2,926 and 2930.78/cm [23]. The presence of carboxylic ion in the biosynthesized solution [25] was revealed by the bands at 2434.90/cm. The OH and CO functionality of the extract plays a responsible role in reducing and stabilizing the nanoparticles [26]. The strong bands at 1,611 and 1,630 cm^{-1} primarily correspond to the CONH stretching associated with the presence of amide groups in the samples while the band at 1,418 cm^{-1} represents the N–H bending vibrational mode. The peaks at about 1,015 and 1,075/cm indicate that there are C–C and C–O-linkages in the samples. Other major IR absorption bands at 1381.65, 1316.67, 777.94, 617.09, 581.78, and 525.98/cm in the spectra of the extract and the nanoparticles represented various functional groups such as ethers, esters, carbonyl (polyol's), or aromatic compounds and alkyl halides that served as reducing and limiting agents during the synthesis of the stable silver nanoparticles. Between the FT-IR spectrum of *Pistacia vera* shell extracts and the FT-IR of biosynthesized nanoparticles, only a minor alteration of the location of the majority of the IR bands is observed. This slight variation in the position of the IR bands of functionalities across the spectrum supported the nanoparticle synthesis using the pista extract.

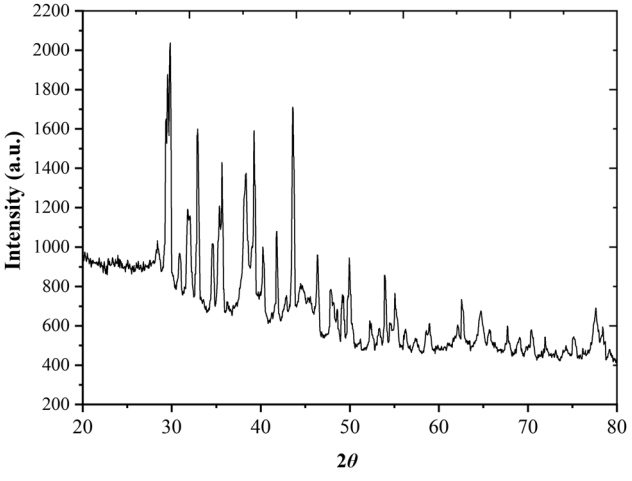

Figure 2: XRD pattern of biosynthesized AgNPs.

3.2 XRD

The X-ray diffraction (XRD) pattern of the green synthesized AgNPs was recorded in the 2θ range 20–80°, as shown in Figure 2. Prominent diffraction peaks at 29.75°, 31.93°, 33.07°, 34.64°, 35.49°, 38.25°, 41.99°, 43.70°, 50.01°, 54.03°, 55.29°, 62.69°, 64.8°, and 77.51° are shown, and the high peak of the XRD pattern signifies active silver composition. In the XRD pattern, characteristic peaks at 29.75°, 38.25°, 43.70°, 64.8°, and 77.51° observed in the experimental diffractogram (Figure 2) are attributed to the silver metal corresponding to *hkl* values at 210, 111, 200, 220, and 311 silver planes. These peaks are related to the face-centered cubic (fcc) crystal lattice structure of silver (JCPDS Nos. 87-0720, 03-0921, and 04-0783). This indicates that the biosynthesized AgNPs are polycrystalline. Similar peak patterns have also been reported [8,10,20] for AgNPs. The average crystallite size of the synthesized AgNPs was found to be around 20 nm using Scherrer's formula. The XRD pattern shows that the silver nanoparticles synthesized by the seed coat extract are crystalline [27,28]. In addition, the extra peaks appearing in the diffractogram may be due to the biomass residue capping of AgNPs [29].

3.3 UV-Vis spectroscopy

To confirm the green synthesis of AgNPs and their stability, UV-Vis analysis was performed. Figure 3b depicts the UV-Vis spectrum of the synthesized AgNPs. It had a ~443 nm absorption band, which is a characteristic band of AgNPs due to the surface plasma resonance (SPR) of silver. The UV-Vis spectrum of the extract of the seed coat (Figure 3a) indicated the presence of polyphenols and flavonoids as reported elsewhere [30]. The absorption peaks at about 260 and 290 nm were attributed to the transition from π to π^* located within the polyphenols as the antioxidant content of the shell.

3.4 Mechanism and stabilization

The polyphenols and flavonoids of the shell play an essential part in the biogenic synthesis of silver nanoparticles by reducing and stabilizing the nanoparticles. They also have other unique properties of adhering to the metal surface to form a coat over AgNPs and thus protect them from aggregation. Based on the GC-MS of pistachio shell extracts published earlier [31–33], featuring important

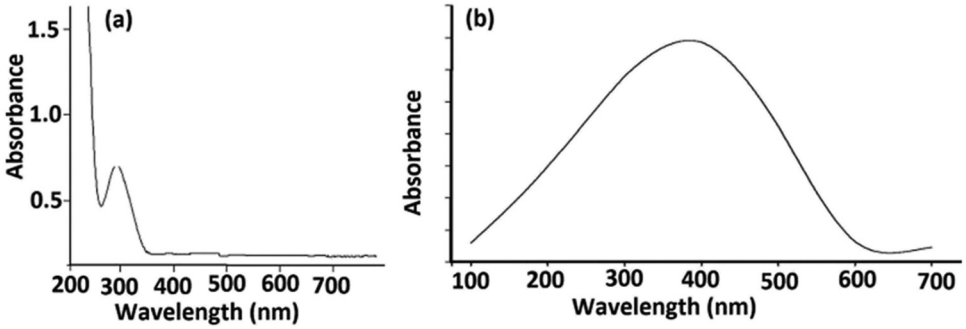

Figure 3: UV-Vis spectrum of (a) the extract of pista shell and (b) AgNPs.

biomolecules such as polyphenols, flavonoids, glycosides, terpenoids, and anthocyanins, these biomolecules – in particular phenolic compounds – play a major role in the reduction of silver ions and prevent them from aggregation; the tentative mechanism (Figure 4) of silver nanoparticle biosynthesis is drawn based on the screening of literature studies [23,34,35].

3.5 SEM, TEM, SAED, and BET studies of biosynthesized AgNPs

SEM data of biosynthesized silver nanoparticles have been used to identify the morphology; it reveals that silver nanoparticles are agglomerated due to induced dehydration but polydispersed with irregular shapes (Figure 5). TEM data confirm the formation of nanoparticles (AgNPs) with irregular shapes, from rectangular to spherical shapes with an average size of 20 nm (Figure 6). BET analysis of AgNPs was performed to know additional information on the surface of nanoparticles obtained from the Brunauer–Emmett–Teller (BET) analysis of the specific surface area. The BET analysis of silver nanoparticles displayed that the surface area of the biogenic AgNPs was 21.73 m^2/g at ambient temperature, and the value obtained from BET correlated with the results obtained from TEM findings (Supplementary file S1). A static volumetric absorption analyzer was also used to calculate the isotherms of N2 absorption–desorption of the biogenic NPs. Figure 6b shows a selected area of the electron diffraction (SAED) pattern of the biogenic AgNPs, which confirms the crystalline nature of the synthesized nanoparticles in the sample, as evidenced by the presence of bright dots.

3.6 Effect of different concentrations of AgNPs and fly ash amendment on plant growth in the pot experiment

Nanoparticle properties, host plant and specific type of nanoparticle interaction, surface coating, size, dosage, exposure time, and a variety of other factors all have an

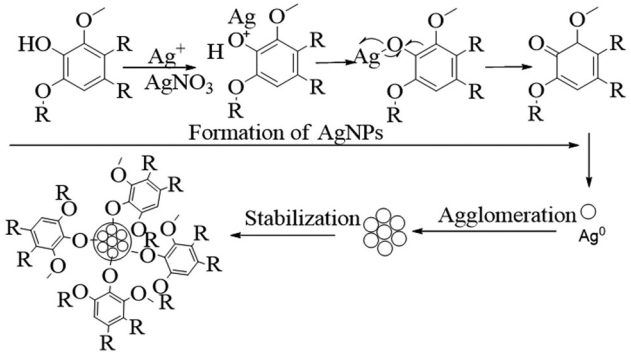

Figure 4: Tentative mechanism and stabilization of biogenic AgNPs.

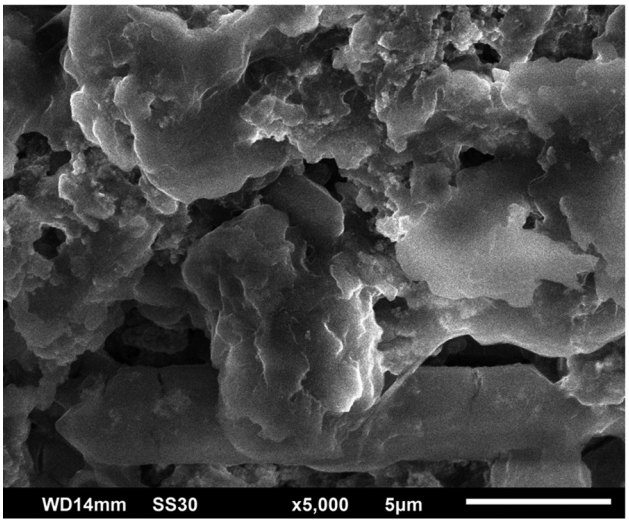

Figure 5: SEM image of the synthesized AgNPs.

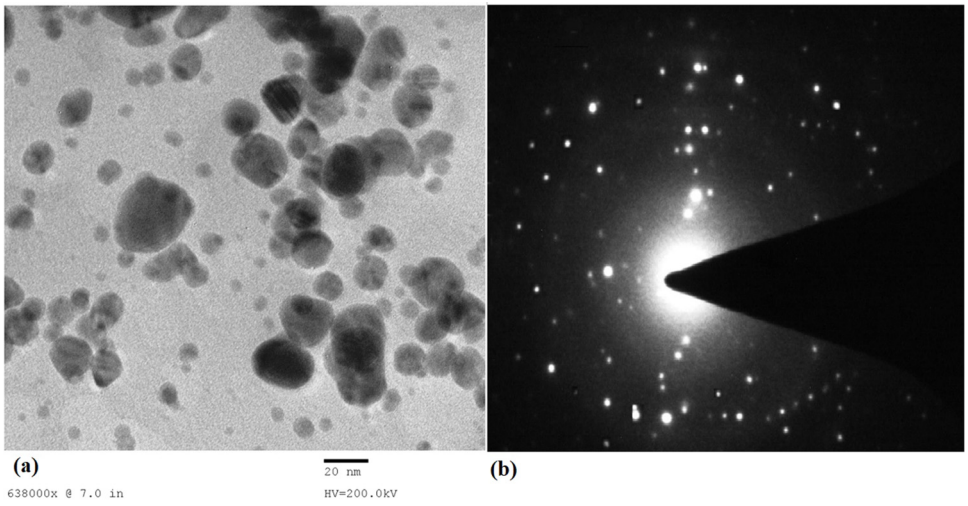

Figure 6: (a) TEM images showing the circular shape of the synthesized AgNPs and (b) the selected area of electron diffraction (SAED) pattern of silver nanoparticles chosen at random.

Figure 7: Eggplants showing the effect of AgNPs and fly ash amendment in soil.

Table 1: Growth profile of eggplants exposed to different concentrations of AgNPs

Treatment	Length (cm)	Fresh weight (g)	Shoot dry weight (g)	Root dry weight (g)	Chlorophyll in fresh leaves (mg/g)	Carotenoid in fresh leaves (mg/g)
C (No AgNPs)	66.96c	50.96c	8.32c	1.75c	1.518c	0.0504d
25 ppm	67.08c	51.12c	8.73c	1.89c	1.527c	0.0517c
50 ppm	70.08b	57.83b	9.98b	2.03b	1.624b	0.0531b
75 ppm	74.93a	62.31a	11.79a	2.38a	1.842a	0.0582a
150 ppm	58.61d	44.75d	7.37d	1.47d	1.281g	0.0428d
300 ppm	55.72f	41.24e	6.08e	1.12e	1.039h	0.0401e
500 ppm	51.24f	38.18f	5.35f	0.96f	0.833i	0.0396f
1,000 ppm	46.56g	34.65g	5.08f	0.91f	0.741j	0.0387g

At $p \leq 0.05$, values within a column and the same type of treatment followed by the same letter do not differ significantly.

impact on their functional expression. Plants are affected by nanoparticles in a number of ways, including morphological and physiological changes. In our research, foliar spraying of eggplant plants with 25, 50, and 75 ppm AgNPs resulted in significant increases in plant growth, chlorophyll, and carotenoid content. The treatment with 50 ppm AgNPs increased the plant length by 4.65% as compared to the control plant. The highest improvement in plant growth occurs after treatment with 75 ppm AgNPs. An increase in the plant length of 11.90% and an increase in the plant fresh weight of 22.27% occur after treatment with 75 ppm AgNPs. A 21.34% increase in the chlorophyll content occurs. The treatment with 75 ppm AgNPs improves the carotenoid content by 15.47% in treated plants. The effect of AgNPs on eggplants is concentration-dependent (Figure 7). Concentrations of 150, 300, 500, and 1,000 ppm

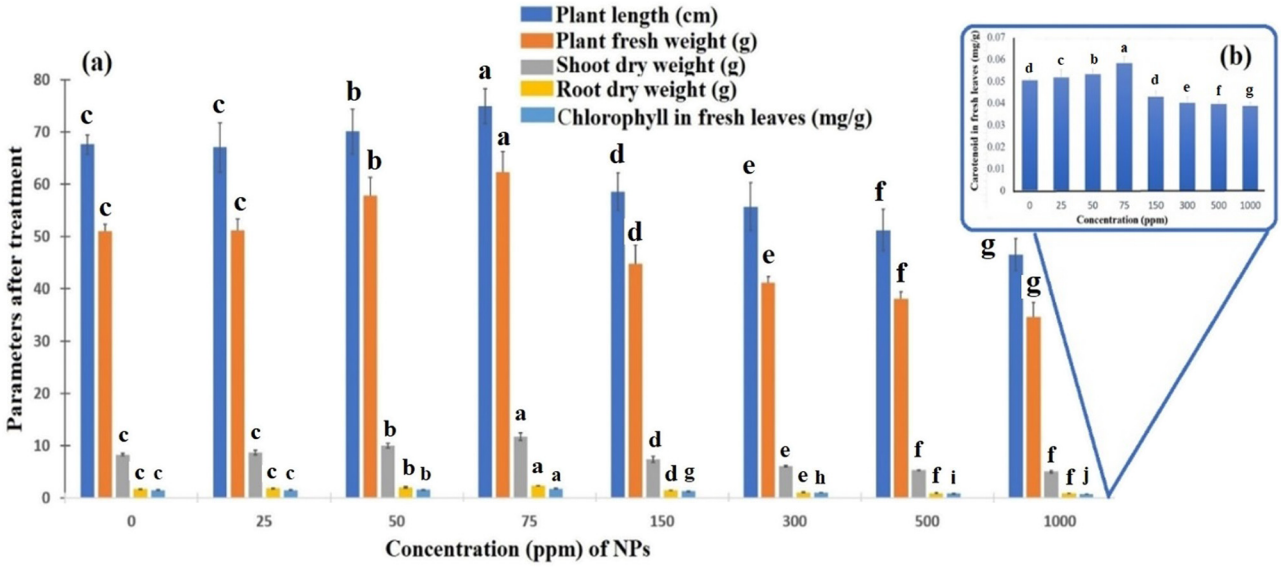

Figure 8: Effect of different concentrations of silver nanoparticles on the growth of the eggplant. C-control (without AgNPs), 25, 50, 75, 150, 300, 500, and 1,000 ppm on the plant length (cm), fresh weight (g), dry weight (g), root dry weight (g), chlorophyll (mg/g), and carotenoid in fresh leaves (mg/g). Graph (b) with fraction data is constructed separately because the graph is not visualized when combined with graph (a) with large data values. There is no significant difference between values within a column and the same type of treatment followed by the same letter. The mean and standard deviation values were used to create the bar graph (Dunnett's test was used as a *post hoc* test). Statistically significant level: $p < 0.05$.

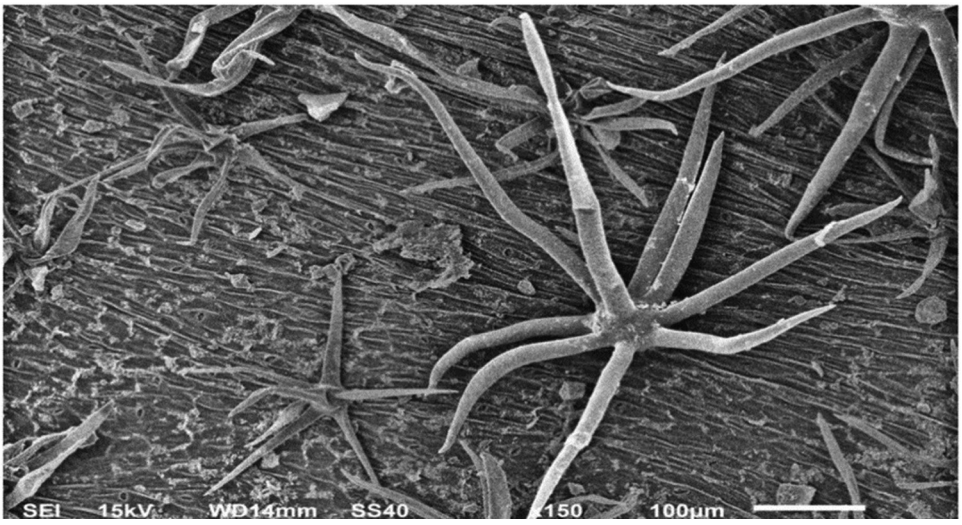

Figure 9: SEM image showing the eggplant leaves sprayed with AgNPs.

were found to be toxic to the eggplant and decreased the plant growth parameters; the highest toxicity was found at 1,000 ppm for the eggplant (Table 1 and Figure 8). The treatment with 1,000 ppm caused a 30.46% reduction in the plant length. The SEM image of the eggplant leaf sprayed with AgNPs is shown in Figure 9. In our experiments, different concentrations of silver nanoparticles were used to determine the effect of nanoparticles (NPs) on the plant growth parameters and photosynthetic pigments, and it was noticed that the eggplant function is adversely affected after a certain limit of the nanoparticle concentration.

Eggplants grown in soil amended with 20% fly ash and sprayed with 75 ppm AgNPs showed a significant increase in the plant growth when compared to plants grown in soil without fly ash (Table 2 and Figure 10). Amendment of the soil with 20% fly ash with 75 ppm AgNPs caused a 10.66% increase in the plant length. However, amendments with 50 and 100% fly ash caused a reduction in the plant growth parameters, and 100% fly ash-amended soil with 75 ppm AgNPs caused a 14.96% decrease in the plant length. A high concentration of AgNPs and also a high concentration of fly ash are not beneficial for the growth of the eggplant. Table 2 shows the positive and negative effects of nanoparticles (NPs) at different concentrations on the plant growth parameters and photosynthetic pigments.

Recent research reported that plant response to AgNPs is dependent on the concentration of AgNPs, which can either enhance or inhibit growth. Exposure to specific concentrations of AgNPs may enhance plant growth compared to nonexposed plants, while higher concentrations have a negative effect on plant growth. AgNPs have a concentration-based effect on eggplants, and a high concentration is toxic for plants. Biosynthesized AgNPs at concentrations of 25, 50, and 75 ppm were found beneficial for eggplant plants but 300, 500, and 1,000 ppm were found to be toxic. Higher concentrations of AgNPs resulted in a reduction of biomass in the Arabidopsis plant, according to Kaveh *et al.* [36]. AgNPs reduced the length of wheat shoots and roots in a dose-dependent manner, as mentioned in the literature [37]. Thuesombat *et al.* discovered that increased AgNP concentrations in jasmine rice reduced seed germination and subsequent seedling growth [38]. The effect of AgNPs on plant morphology and physiology is determined by their size and shape. Foliar application of AgNPs at different concentrations (20, 40, and 60 mg/L) was found to improve fenugreek plant growth parameters [39]. On mung beans, similar results of improving the role of AgNP treatments were obtained [40]. Growth-promoting AgNP activity on the wheat plant was also registered [41]. *Brassica juncea*, common bean, and corn all benefit

Table 2: Effect of fly ash and AgNPs on the eggplant plant growth

Treatment	Length (cm)	Fresh weight (g)	Shoot dry weight (g)	Root dry weight (g)	Chlorophyll in fresh leaves (mg/g)	Carotenoid in fresh leaves (mg/g)
0% FA + 75 ppm AgNPs	74.93a*	62.31a	11.79a	2.38a	1.717c	0.050cd
20% FA + 75 ppm AgNPs	82.92a	69.41a	14.46a	2.91a	1.842c	0.0582cd
50% FA + 75 ppm AgNPs	70.48c	60.43c	12.21c	1.93c	1.477d	0.046bc
100% FA + 75 ppm AgNPs	63.72d	42.72e	10.04d	1.18e	1.397e	0.039e

*Values within a column having the same letter are not significantly different at $p \leq 0.05$. a a c e a a c d.

from AgNPs in terms of plant growth and biochemical attributes such as chlorophyll, carbohydrate/protein contents, and antioxidant enzymes [42,43]. Silver is an impressive growth simulator as reported in the literature elsewhere [44]. Furthermore, Krishnaraj *et al.* [45] discovered that biosynthesized AgNPs influenced seed germination and induced protein and carbohydrate synthesis in *Bacopa monnieri*. In agriculture, AgNPs were developed as plant-growth stimulators [46] and the report of Khan and Siddiqui [47] states that 25% fly ash-amendment in the soil is better for plant growth, and 50% fly ash amendment and 100% fly ash are harmful to the eggplant plant growth. It is evident from previous studies that AgNPs can affect the plants' growth attributes and metabolic processes. It was reported that AgNPs improved seed germination in pearl millet [48]. Parveen and Rao [34] reported that AgNPs can increase the germination rate, vigor index, and germination index in *Brassica juncea*. Sadak [39] found that silver nanoparticles could improve fenugreek plant (*Trigonella foenum-graecum*) growth, yield, and some biochemical aspects. AgNPs can be used for the breeding of chrysanthemum plants. Treatment of AgNPs (20 ppm) could improve the carotenoid content and induce genetic and phenotypic variation in the chrysanthemum plant [49]. An in-depth investigation is needed to understand the actual mechanism of the mediating effects of AgNPs on crops. Danish *et al.* [50] synthesized silver nanoparticles (AgNPs) from plants and found that the 50 ppm AgNP treatment in *Trachyspermum ammi* L. plant improved plant growth, biochemical, and antioxidant enzyme activities. They also reported that the AgNP treatment reduced the nematode infection in treated plants.

3.7 Statistical analysis

The results were provided as mean ± SD and expressed as an average for the measurement. Test values, degrees of freedom, and p values were used to examine statistical differences and significant means in the experimental data. In all statistical studies, the significant difference was determined using the Dunnett test at a level of 0.05 (or 0.01), which is provided in the supplementary information under statistical analysis. Each experimental value was differentiated to its corresponding control value. In nanoparticles-treated plants, a differential correlation pattern was noted between various concentrations of nanoparticles and parameters for plant growth such as plant length (cm), plant fresh weight (g), shoot

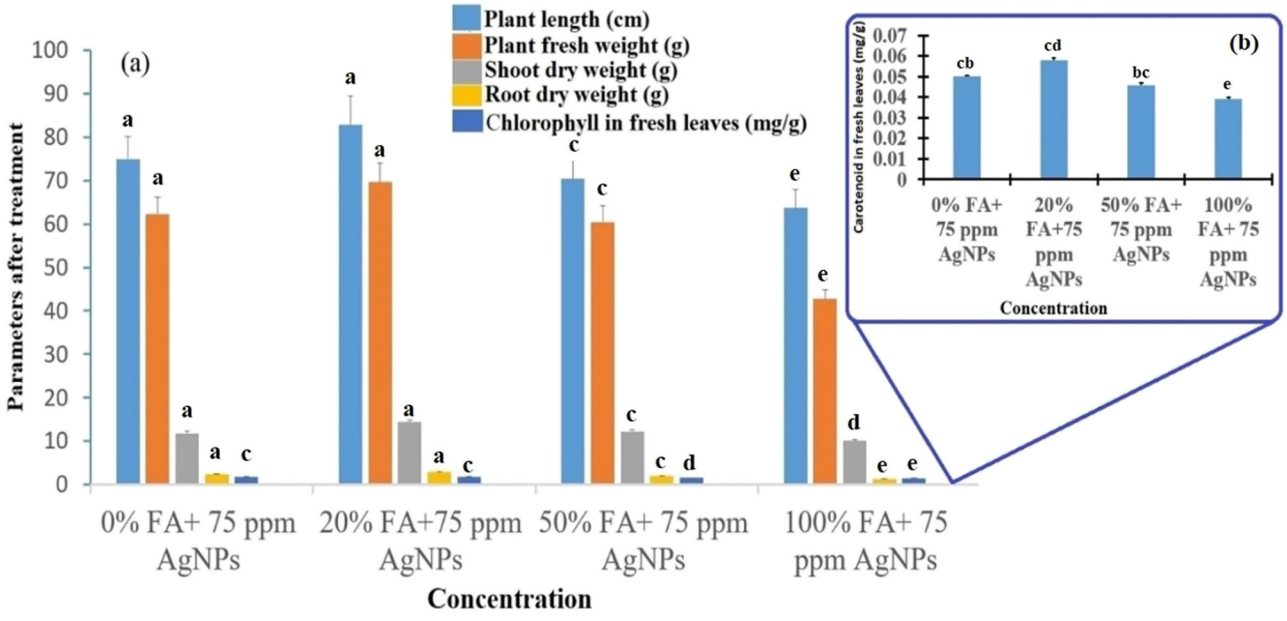

Figure 10: Effect of different concentrations of fly ash with an effective concentration of silver nanoparticles (75 ppm) on the growth of the eggplant plant. 0% FA + 75 ppm AgNPs, 20% FA + 75 ppm AgNPs, 50% FA + 75 ppm AgNPs and 100% FA + 75 ppm AgNPs on the plant length (cm), plant fresh weight (g), shoot dry weight (g), root dry weight (g), chlorophyll in fresh leaves (mg/g), and (b) carotenoid in fresh leaves (mg/g). Graph (b) with fraction data is constructed separately because the graph is not visualized when combined with graph (a) with large data values. The mean and standard deviation values were used to create the bar graph (Dunnett's test was used as a *post hoc* test). Statistically significant level: $p < 0.05$.

dry weight (g), root dry weight (g), chlorophyll in fresh leaves (mg/g), and carotenoid in fresh leaves (mg/g). The total chlorophyll in fresh leaves (r^2 = 0.9859), carotenoid in fresh leaves (r^2 = 0.9116), and root dry weight (r^2 = 0.9787) showed positive correlation at different concentrations of silver nanoparticles. However, different concentrations of fly ash with a fixed concentration of silver nanoparticles (75 ppm) show significant difference on various factors of plant growth as indicated by positive *R* squared values for the plant length (r^2 = 0.7246), plant fresh weight (r^2 = 0.9160), shoot dry weight (r^2 = 0.9551), root dry weight (r^2 = 0.9934), chlorophyll in fresh leaves (r^2 = 0.9508), and carotenoid in fresh leaves (r^2 = 0.9871). The plant length, plant fresh weight, and shoot dry weight did not have a significant difference mean with different concentrations of silver nanoparticles (see supplementary information S1).

4 Conclusion

In this study, 10 mL of the pista seed coat waste extract was found to be suitable for harvesting a larger quantity of AgNPs within 30 min. The results explained in this article are therefore novel, which could emerge as a better alternative to the synthesis of AgNPs using waste plant materials. Biologically active compounds such as alkaloids, amino acids, flavonoids, and glycosides were identified from the extracts by the study of functional groups: –OH, –NH, –C═O, –COOH, and –CONH using IR spectrum; previous reports of GC-MS and these phytochemicals may be responsible for the rapid reduction of Ag+, leading to the AgNP formation. Morphological and particle sizes were confirmed using various techniques, such as SEM, TEM, XRD, and BET, and were found to possess polydispersed irregular shapes from rectangular to spherical shapes with an average size of 20 nm. The BET study also confirmed the surface area of biogenic AgNPs to be 21.73 m^2/g at ambient temperature. The effect of AgNPs on the eggplant has been shown to enhance the growth of the eggplant at low concentrations but higher concentrations are toxic to the eggplant plant: 20% fly ash amendment in soil with spraying 75 ppm AgNPs was found most effective in improving the growth of the eggplant and 50% fly ash amendment in the soil was found to be less effective. Further research is required to determine the degree of toxicity, and the mechanistic approach of AgNPs to plant growth for field applications is important for further use.

Funding information: Walaa Alsanie would like to acknowledge TURSP (2020/53).

Author contributions: All authors have accepted responsibility for the entire content of this manuscript and approved its submission.

Conflict of interest: The authors declare no conflict of interest.

References

[1] Mohseniazar M, Barin M, Zarredar H, Alizadeh S, Shanehbandi D. Potential of microalgae and lactobacilli in biosynthesis of silver nanoparticles. BioImpacts. 2011;1:149–52.
[2] Pal SL, Jana U, Manna PK, Mohanta GP, Manavalan R. Nanoparticle: an overview of preparation and characterization. J Appl Pharm Sci. 2011;1(6):228–34.
[3] Feynman RP. There's plenty of room at the bottom. Eng Sci. 1960;23:22–36.
[4] Azmir J, Zaidul IS, Rahman MM, Sharif KM, Mohamed A, Sahena F, et al. Techniques for extraction of bioactive compounds from plant materials: a review. J Food Eng. 2013;117:426–36.
[5] Pérez C, del Castillo ML, Gil C, Blanch GP, Flores G. Supercritical fluid extraction of grape seeds: extract chemical composition, antioxidant activity and inhibition of nitrite production in LPS-stimulated Raw 264.7 cells. Food Funct. 2015;6:2607–13.
[6] de Barros CH, Cruz GC, Mayrink W, Tasic L. Bio-based synthesis of silver nanoparticles from orange waste: effects of distinct biomolecule coatings on size, morphology, and antimicrobial activity. Nanotechnol Sci Appl. 2018;11:1–14.
[7] Vance ME, Kuiken T, Vejerano EP, McGinnis SP, Hochella Jr MF, Rejeski D, et al. Nanotechnology in the real world: redeveloping the nanomaterial consumer products inventory. Beilstein J Nanotechnol. 2015;6:1769–80.
[8] Khan M, Khan AU, Alam MJ, Park S, Alam M. Biosynthesis of silver nanoparticles and its application against phytopathogenic bacterium and fungus. Int J Environ Anal Chem. 2020;100(12):1390–401.
[9] Kaur J, Singh J, Rawat M. An efficient and blistering reduction of 4-nitrophenol by green synthesized silver nanoparticles. SN Appl Sci. 2019;1:1–6.
[10] Khan AU, Khan M, Khan MM. Antifungal and antibacterial assay by silver nanoparticles synthesized from aqueous leaf extract of Trigonella foenum-graecum. BioNanoScience. 2019;9:597–602.
[11] Valli JS, Vaseeharan B. Biosynthesis of silver nanoparticles by Cissus quadrangularis extracts. Mater Lett. 2012;82:171–3.
[12] Kumar DA, Palanichamy V, Roopan SM. Green synthesis of silver nanoparticles using Alternanthera dentata leaf extract at room temperature and their antimicrobial activity. Spectrochim Acta A. 2014;127:168–71.

[13] Verma SK, Das AK, Patel MK, Shah A, Kumar V, Gantait S. Engineered nanomaterials for plant growth and development: a perspective analysis. Sci Total Environ. 2018;630:1413–35.
[14] Aslani F, Bagheri S, Julkapli NM, Juraimi AS, Sadat F, Hashemi G, et al. Effects of engineered nanomaterials on plants growth: an overview. Sci World J. 2014;2014:641759.
[15] Khan M, Khan AU, Hasan MA, Yadav KK, Pinto M, Malik N, et al. Agro-nanotechnology as an emerging field: a novel sustainable approach for improving plant growth by reducing biotic stress. Appl Sci. 2021;11:2282.
[16] Glance. Horticultural Statistics Horticulture Statistics Division Department of Agriculture. Cooperation & Farmers' Welfare Ministry of Agriculture and Farmers' Welfare Government of India; 2018.
[17] Izabela J, Oleszczuk P. Influence of soil type and environmental conditions on ZnO, TiO_2 and Ni nanoparticles phytotoxicity. Chemosphere. 2013;92:91–9.
[18] Khodakovskaya MV, Silva K, Nedosekin DA, Dervishi E, Biris AS, Shashkov EV, et al. Complex genetic, photothermal, and photoacoustic analysis of nanoparticle-plant interactions. Proc Natl Acad Sci. 2011;108:1028–33.
[19] Wang LJ, Guo ZM, Li TJ, Li M. The nano structure SiO_2 in the plants. Chin Sci Bull. 2001;46:625–31.
[20] Khan M, Khan AU, Bogdanchikova N, Garibo D. Antibacterial and antifungal studies of biosynthesized silver nanoparticles against plant parasitic nematode *Meloidogyne incognita,* plant pathogens ralstonia solanacearum and fusarium oxysporum. Molecules. 2021;26:2462.
[21] Mackinney G. Criteria for purity of chlorophyll preparations. J Biol Chem. 1940;132:91–109.
[22] Maclachlan S, Saul Z. Plastid structure, chlorophyll concentration, and free amino acid composition of a chlorophyll mutant of barley. Can J Bot. 1963;41:1053–62.
[23] Vanaja M, Gnanajobitha G, Paulkumar K, Rajeshkumar S, Malarkodi C, Annadurai G. Phytosynthesis of silver nanoparticles by Cissus quadrangularis: influence of physicochemical factors. J Nanostruct Chem. 2013;3:1–8.
[24] Suresh S, Karthikeyan S, Jayamoorthy K. FTIR and multivariate analysis to study the effect of bulk and nano copper oxide on peanut plant leaves. J Sci Adv Mater Devices. 2016;1:343–50.
[25] Ajitha BY, Reddy AK, Reddy PS. Biogenic nano-scale silver particles by Tephrosia purpurea leaf extract and their inborn antimicrobial activity. Spectrochim Acta A. 2014;121:164–72.
[26] Sre PR, Reka RM, Poovazhagi R, Arul Kumar M, Murugesan K. Antibacterial and cytotoxic effect of biologically synthesized silver nanoparticles using aqueous root extract of Erythrina indica lam. Spectrochim Acta A. 2015;135:1137–44.
[27] Venil CK, Malathi M, Velmurugan P, Renuka Devi P. Green synthesis of silver nanoparticles using canthaxanthin from Dietziamaris AURCCBT01 and their cytotoxic properties against human keratinocyte cell line. J Appl Microbiol. 2021;130:1730–44.
[28] Anigol LB, Charantimath JS, Gurubasavaraj PM. Effect of concentration and pH on the size of silver nanoparticles synthesized by green chemistry. Org Med Chem Int J. 2017;3:1–5.
[29] Mahiuddin M, Saha P, Ochiai B. Green synthesis and catalytic activity of silver nanoparticles based on piper chaba stem extracts. Nanomaterials. 2020;10:1777.
[30] Taghizadeh A, Rad-Moghadam K. Green fabrication of Cu/pistachio shell nanocomposite using Pistacia Vera L. hull: an efficient catalyst for expedient reduction of 4-nitrophenol and organic dyes. J Clean Prod. 2018;198:1105–19.
[31] Toldrá F, Nollet LM, editors. Handbook of dairy foods analysis. Oxon, OX14RN. CRC Press; 2021. p. 29.
[32] Xinyuan J, Yuanyuan L, Zhong G, An M, Zecai H, Suwen Y. Pyrolysis characteristics and correlation analysis with the major components of seven kinds of nutshell. Sci Silvae Sin. 2015;51:79–86.
[33] Bordbar M, Mortazavimanesh N. Biosynthesis of waste pistachio shell supported silver nanoparticles for the catalytic reduction processes. IET Nanobiotechnol. 2018;12:939–45.
[34] Parveen A, Rao S. Effect of nanosilver on seed germination and seedling growth in Pennisetum glaucum. J Clust Sci. 2015;26:693–701.
[35] Zafar S, Zafar A. Biosynthesis and characterization of silver nanoparticles using Phoenix dactylifera fruits extract and their in vitro antimicrobial and cytotoxic effects. Open Biotechnol J. 2019;13:37–46.
[36] Kaveh R, Yue-Sheng L, Ranjbar S, Tehrani R, Brueck CL, Aken BV. Changes in Arabidopsis thaliana gene expression in response to silver nanoparticles and silver ions. Environ Sci Technol. 2013;2013(47):10637–44.
[37] Dimkpa CO, McLean JE, Martineau N, Britt DW, Haverkamp R, Anderson AJ. Silver nanoparticles disrupt wheat (Triticum aestivum L.) growth in a sand matrix. Environ Sci Technol. 2013;47:1082–90.
[38] Thuesombat P, Hannongbua S, Akasit S, Chadchawan S. Effect of silver nanoparticles on rice (Oryza sativa L. cv. KDML 105) seed germination and seedling growth. Ecotoxicol Environ Saf. 2014;104:302–9.
[39] Sadak MS. Impact of silver nanoparticles on plant growth, some biochemical aspects, and yield of fenugreek plant (Trigonella foenum-graecum). Bull Natl Res Cent. 2019;43:1–6.
[40] Saeideh N, Rashid J. Effect of silver nanoparticles and Pb $(NO_3)_2$ on the yield and chemical composition of mung bean (Vigna radiata). J Stress Physiol Biochem. 2014;10:316–25.
[41] Razzaq A, Ammara R, Jhanzab HM, Mahmood T, Hafeez A, Hussain SA. novel nanomaterial to enhance growth and yield of wheat. J Nanosci Technol. 2016;2:55–8.
[42] Salama HM. Effects of silver nanoparticles in some crop plants, common bean (Phaseolus vulgaris L.) and corn (Zea mays L.). Int Res J Biotechnol. 2012;3:190–7.
[43] Sharma P, Bhatt D, Zaidi MG, Saradhi PP, Khanna PK, Arora S. Silver nanoparticle-mediated enhancement in growth and antioxidant status of Brassica juncea. Appl Biochem Biotechnol. 2012;167:2225–33.
[44] Sharon M, Choudhary AK, Kumar R. Nanotechnology in agricultural diseases and food safety. J Phytol. 2010;2(4):83–92.
[45] Krishnaraj C, Jagan EG, Ramachandran R, Abirami SM, Mohan N, Kalaichelvan PT. Effect of biologically synthesized silver nanoparticles on Bacopa monnieri (Linn.) Wettst. plant growth metabolism. Process Biochem. 2012;47(4):651–8.
[46] Monica RC, Cremonini R. Nanoparticles and higher plants. Caryologia. 2009;62:161–5.
[47] Khan M, Siddiqui ZA. Effects of fly ash amendments, Ralstonia solanacearum, Meloidogyne incognita and Phomopsis vexans on the growth of Solanum melongena. Acta Phytopathol Entomol Hung. 2017;52:145–56.
[48] Khan I, Raza MA, Awan SA, Shah GA, Rizwan M, Ali B, et al. Amelioration of salt induced toxicity in pearl millet by seed priming with silver nanoparticles (AgNPs): the oxidative

damage, antioxidant enzymes and ions uptake are major determinants of salt tolerant capacity. Plant Physiol Biochem. 2020;156:221–32.
[49] Tymoszuk A, Kulus D. Silver nanoparticles induce genetic, biochemical, and phenotype variation in chrysanthemum. Plant Cell Tissue Organ Cult. 2020;143:331–44.
[50] Danish M, Altaf M, Robab MI, Shahid M, Manoharadas S, Hussain SA, et al. Green synthesized silver nanoparticles mitigate biotic stress induced by meloidogyne incognita in Trachyspermumammi (L.) by improving growth, biochemical, and antioxidant enzyme activities. ACS Omega. 2021;6:11389–403.